

Marine spatial planning techniques with a case study on wave-powered offshore aquaculture farms

Gabriel Ewig^{a,*}, Arezoo Hasankhani^b, Eugene Won^c, Maha Haji^a

^a*Sibley School of Mechanical and Aerospace Engineering, Cornell University, Ithaca, NY, 14853, USA*

^b*Department of Electrical and Computer Engineering, University of New Hampshire, Durham, NH, 03824, USA*

^c*Department of Animal Science, Cornell University, Ithaca, NY, 14853, USA*

Abstract

As emerging marine technologies lead to the development of new infrastructure across the ocean, they enter an environment that existing ecosystems and industries already rely on. Although necessary to provide sustainable sources of energy and food, careful planning will be important to make informed decisions and avoid conflicts. This paper examines several techniques used for marine spatial planning, an approach for analyzing and planning the use of marine resources. Using open-source software including QGIS and Python, the potential for developing offshore aquaculture farms powered by a reference model wave energy converter from the Sandia National Labs, the RM3, along the Northeast coast of the United States is assessed and several feasible sites are identified. The optimal site, located at 43.7°N 68.9°W along the coast of Maine, has a total cost for a 5-pen farm of \$56.8M, annual fish yield of 676 tonnes, and a levelized cost of fish of \$9.23 per kilogram. Overall trends indicate that the cost greatly decreases with distance to shore due to the greater availability of wave energy and that conflicts and environmental constraints significantly limit the number of feasible sites in this region.

Keywords: marine spatial planning, fisheries, offshore aquaculture, wave energy, gis, python

1. Introduction

Oceans have long been a source of opportunity, and conflict, for the communities and industries along their shores. This rich environment, first used as a source of food and for recreation, has since been utilized by other offshore activities including mineral extraction, shipping, aquaculture, and most recently, offshore renewable energy (ORE) systems. Even before the expansion of renewable energy, interactions between different industries led to challenging situations between fisheries and other stakeholders with varying degrees of resolution. Arbo and Thủy (2016), for example, researched disputes between the oil industry and fisheries in Norway and Vietnam. In Norway, the two industries were able to reach a

*Corresponding author

Email addresses: gre27@cornell.edu (Gabriel Ewig), arezoo.hasankhani@unh.edu (Arezoo Hasankhani), etw36@cornell.edu (Eugene Won), maha@cornell.edu (Maha Haji)

common agreement to collaborate and work together with an integrated management plan in the Barents Sea, while in Vietnam the two industries have continued to face challenging conflicts. Another study by Andrews et al. (2021) examined the offshore oil industry’s adverse impacts on the environment, small-scale fisheries, and coastal community livelihood. Conflicts involving fisheries are further complicated by uncontrolled fishing activities and overlap between recreational and commercial fisheries, which threaten fish stocks and the overall health of the ocean (Bess and Rallapudi, 2007).

Entering this mix is the emerging industry of offshore aquaculture, which has the potential to provide a more sustainable and protein-rich source of food for the growing population (NOAA Fisheries, 2023). Compared to conventional aquaculture, offshore aquaculture farms raise fish in the open ocean instead of sheltered bays or onshore tanks. Existing literature by researchers including Gentry et al. (2017), Weiss et al. (2018), Brugere (2006), and Bishwajit (2014) has brought to light challenges and opportunities for aquaculture farms, including the potential for significant expansion in many parts of the world including Southeast Asia, Australia, North America, and South America. Many of these studies, and particularly Longdill et al. (2008), look specifically at the impact on the local environment and how different environmental factors and the siting of farms can change the effects of pollution and other negative disturbances. However, few consider the energy source of the farm, which is often diesel generators, and the potential ways to mitigate the environmental impacts of the associated fossil fuel use.

High ORE growth in response to climate change has created new challenges for many fisheries that currently use the same waters. Stelzenmüller et al. (2022), studied the impacts of ORE development in the North Sea and the socioeconomic effects on fisheries in that region. Although they find that conflicts exist currently and are ongoing, they predict increasing friction between fisheries and ORE activities after 2025. Some work does show promising signs for the collaboration between existing fisheries and the expanding ORE industry, particularly when coastal communities are brought into the planning process early on. The Block Island Wind Farm, for example, was able to work with local communities and fisheries and decided to change certain plans, including the placement of the turbines, in response to community input (Firestone et al., 2020; ten Brink and Dalton, 2018).

The opportunity to co-locate offshore activities together is another promising solution for managing the increasingly congested ocean. Two industries with the potential for co-location are ORE systems and offshore aquaculture farms, where an ORE system can power the farm and potentially shield it from incoming waves. Several studies exist discussing the feasibility of co-locating offshore wind farms to make more efficient use of ocean space including Buck et al. (2004), Buck et al. (2008), Gimpel et al. (2015), and Wever et al. (2015). Co-location with wave energy converters (WECs) to form a wave-powered aquaculture farm (WPAF) is a particularly interesting option that may be a better match due to a WEC’s smaller size and power output, which is closer in scale to the needs of an aquaculture farm. In Garavelli et al. (2022), the authors analyzed the feasibility of this co-location in the United States and identified California and Hawaii as promising sites for future deployment. Co-located WPAFs have also been investigated along the Portuguese coastline, where six different types of WECs have been compared in terms of cost, energy coverage, and capacity factor (Clemente et al., 2023). Whiting et al. (2023) and Silva et al. (2018) have also investigated the near and far-field effects of wave energy which has the potential to dampen waves as they approach

an aquaculture farm, although this is still an area of active research.

Previous work by the authors of this paper has developed the groundwork for basic conceptual design and optimization of a WPAF (Hasankhani et al., 2023a) and initial attempts to site such a project in the Northeast United States (Hasankhani et al., 2023b). However, a comprehensive framework for marine spatial planning (MSP) using QGIS and Python, specifically one that considers conflicts with other offshore activities and the environmental and geographic requirements for a WPAF, has yet to be detailed. This paper provides a detailed and general framework for the preprocessing and analysis needed for MSP, and applies those techniques alongside an updated cost model to the question of offshore aquaculture siting.

Using these techniques, the authors of this paper aim to assess the potential to integrate wave power into the farm setup, analyze the potential conflicts and environmental constraints that such a farm might face, and provide suggestions for the development of such a farm in the Northeast United States. The farm is modeled using Atlantic salmon, the reference model three (RM3) WEC, and submersible net pens like those from Innovasea, as explained in section 2. By beginning with large-scale mapping techniques, promising sites in the region of interest are identified, and details of the overall considerations that must be made when co-locating wave energy converters and aquaculture farms are revealed. Further integration with Python allows GIS information to be used in a more complex modeling process that includes an objective function to identify cost-effective sites while meeting several constraints. These techniques exemplify the ways that GIS information and modeling could be integrated into a wide range of MSP processes to improve the understanding of the oceanic environment, pick out overall trends relevant to a project, and initiate early engagement with stakeholders to avoid or mitigate potential issues.

Each section of the paper aims to present general information about the MSP process in addition to the specific ways that these methods are applied to the case study of a WPAF. Section 2 provides a brief overview of the problem formulation for the application of MSP techniques to a WPAF in the Northeast United States. Section 3 continues with considerations for selecting a scope and data sets for a problem, followed by sections 4 and 5 which detail the methods used in both Python and QGIS to process the data sets and model different potential WPAF sites. Finally, sections 6 and 7 present the results and discuss observed trends. The Python code referenced in this paper is available in a repository on the SEA Lab GitHub at <https://github.com/symbiotic-engineering/aquaculture> and the relevant data files are hosted on Zenodo at <https://zenodo.org/records/10140826>.

2. Problem formulation

The MSP techniques examined in this paper can be used for a variety of purposes, such as the siting of offshore energy infrastructure and identifying potential conflicts between stakeholders. These techniques are potentially applicable to a wide array of offshore developments, but the specific application of MSP to a WPAF in the Northeast United States is the focus on this study. Figure 1 provides an overview of the process used for this study and other potential applications.

Offshore aquaculture has the potential to provide a sustainable source of seafood for the world’s growing population. By taking advantage of more space and higher current speeds

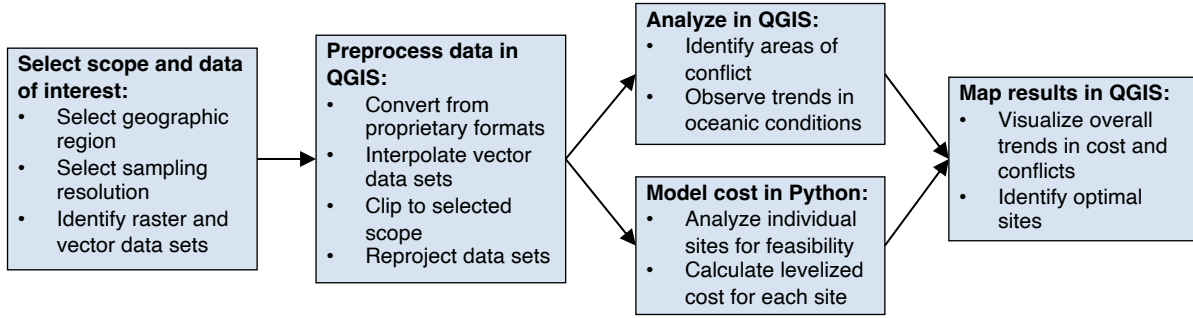


Figure 1: Flowchart describing the marine spatial planning process used, including selecting the scope and data, preprocessing data sets, analysis in both QGIS and Python, and visualizing results.

further from shore, offshore farms could reduce local environmental impact and expand production. However, the energy demand for necessary equipment like lights and feeders in current designs is supplied by diesel generators. This fossil fuel based source of power further pollutes the environment and requires a regular diesel supply from shore. The use of WECs alongside aquaculture farms has the potential to replace diesel generators and alleviate some of these issues, although many of the local environmental concerns still need to be addressed. In order to investigate this potential co-location, the following points are considered to identify optimal sites in the Northeast United states:

- the deployment location should meet the environmental requirements of Atlantic salmon including temperature, salinity, dissolved oxygen, and current speed;
- the deployment location should have enough wave power density to power the aquaculture farm, as determined by data on significant wave height and wave energy period;
- the WPAF should be installed in a location with a suitable depth for mooring necessary equipment;
- the WPAF should avoid conflicts with existing offshore activities such as commercial fisheries and wind lease areas; and
- feasible sites should be evaluated for location-dependent costs to minimize the cost of the WPAF.

The modeled WPAF includes five cylindrical net pens of 30 m diameter and 15 m height, each with a fish stocking density of $15 \frac{\text{kg}}{\text{m}^3}$. The net pen design is similar to those designed by Innovasea, and will be stocked with Atlantic salmon, a common and in-demand species with similar biological needs to steelhead trout, as the target species. The WECs used to power the farm will be the Reference Model 3 (RM3) as designed by Sandia National Laboratories. The RM3 WEC is a two-body heaving point absorber with a top float that moves relative to a vertical column and reaction place when excited by waves. This mechanical energy from ocean waves is converted into electrical energy through a power take-off (PTO) system and a generator within the WEC. The RM3 has a height of 30 m, float diameter of 20m, and a

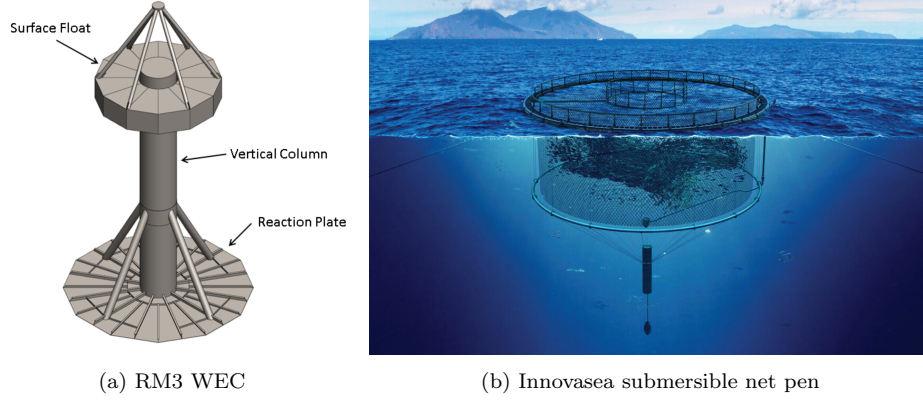


Figure 2: Reference model 3 (RM3) wave energy converter (Neary et al., 2014), and Innovasea submersible net pen considered in this study (Innovasea, 2023).

rated capacity of 286 kW (Neary et al., 2014). Per discussion with aquaculture stakeholders, a spacing of 150 m between the net pens is considered to provide enough space for the mooring and vessel operation. Additionally, the spacing between WECs is considered twice the WEC diameter to avoid any destructive wave interaction and reduction in the generated power (Zhong and Yeung, 2019). Two feed barges are also required to enable automatic fish feeding; each barge has six feed lines and a capacity of 200 metric tons (Scale Aquaculture AS, 2019). Travel to the net pens using ships is scheduled weekly to restock the feed barges and check the aquaculture farm.

3. Scope and data selection

3.1. Study scope

This study focuses on waters along the Atlantic coast of the Northeastern United States. The region is home to several large fisheries, and the industry holds important historical and cultural significance in the area. Overfishing and environmental changes over the past decades, however, have greatly diminished fish stocks leading to record lows in annual catches of cod and other species (Whittle, 2022). The region is also home to several aquaculture operations, although the authors are not aware of any currently located far offshore as suggested in this study. Northeast Sea Grant defines the Northeast as the states of Maine, New Hampshire, Massachusetts, Rhode Island, Connecticut, and New York (Northeast Sea Grant, 2022), which are therefore the main focus of this study. However, to include all regions that are easily accessible from ports in these states, this study uses a slightly larger scope which also includes Delaware and New Jersey. The study includes both state waters, within 5.6km (3 nautical miles) of shore, and federal waters, within 370km (200 nautical miles) of shore, as shown in figure 3. This region is roughly bounded by 38.40°N 75.80°W and 45.20°N 65.70°W.

There are several approaches to evaluating complex models across a large region, depending on the needs of a project. Projects aiming to identify individual optimal sites may benefit from optimization techniques such as gradient descent that search for locations that minimize an objective function such as cost. For this study, however, a brute-force approach

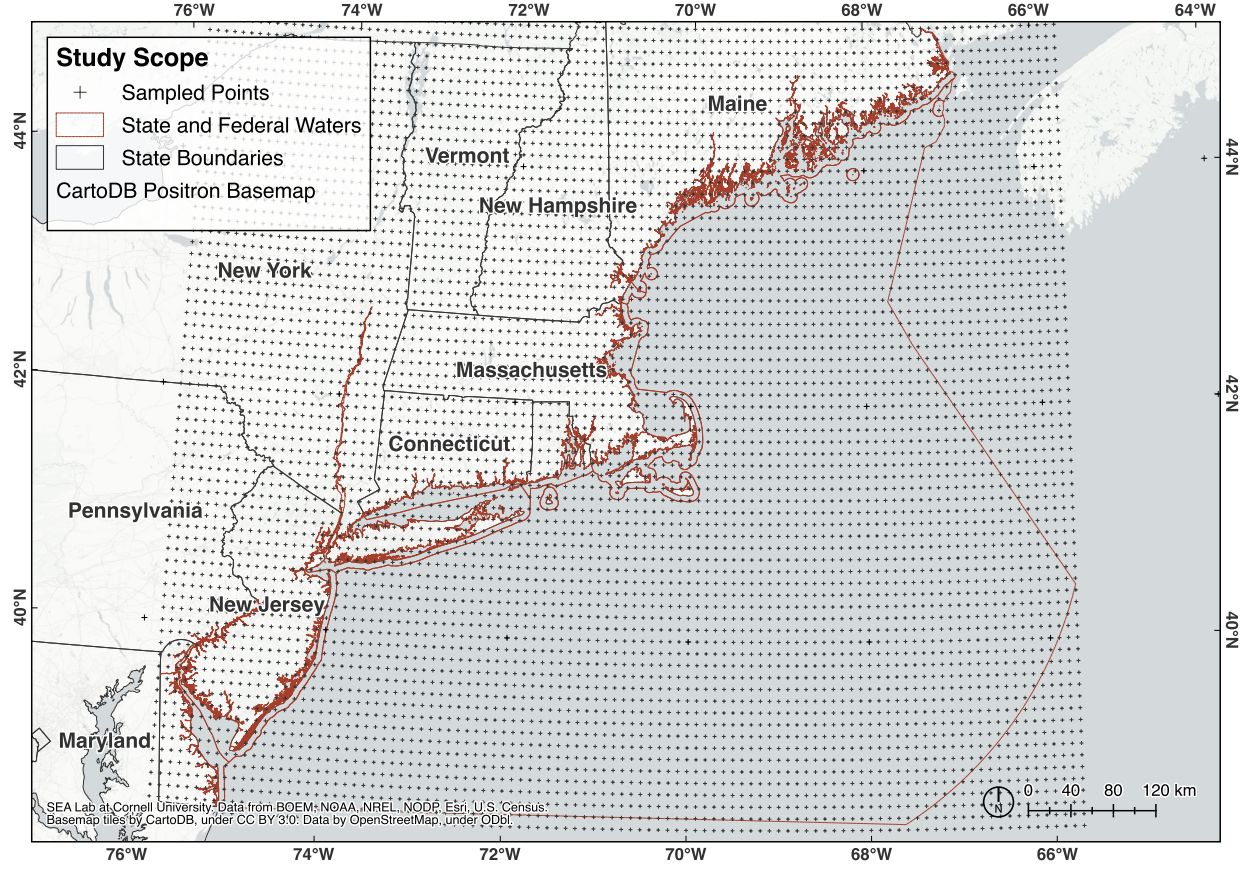


Figure 3: Selected region of Northeastern United States including state and federal waters, along with the 0.1° grid of sampled points (points over land are excluded early in analysis).

is used to allow the entire region to be evaluated so that overall trends can easily be identified. Unlike an optimization approach which strategically searches for a minimum, the brute-force approach evaluates every location at a set interval across the region. Although more time-consuming, the results of this approach provides a more complete understanding of the entire region. The results using this approach are achieved in a reasonable time frame, under an hour, for the current model, however a more complex model may necessitate a different approach to optimization. The interval at which sites are evaluated with this approach determines the “resolution” of the results, which is limited by how much processing time is practical and the lowest resolution of the data sets used in the study. Some common properties like bathymetry have very high-resolution data sets available, while others may be lower resolution or limited to smaller areas. For this study, a resolution of 0.1° longitude and latitude (roughly 10km in this region) is selected to balance the need for precision while not being overly demanding of computational time. This is slightly lower than the most limiting data sets of wave conditions, which have a resolution of about 0.067° . Figure 3 shows the points sampled at this resolution alongside the state and federal waters included in the study scope. While this resolution provides general trends across the entire region, a higher resolution pass would be necessary for later stages of planning, especially once a more specific region of interest can be identified. Table 1 includes the resolution of individual data

files, which indicate the highest resolution that could be achieved before other data sources become necessary.

3.2. Sources of data

GIS data types fall into two general types: raster and vector data sets. Raster data sets provide pixels of continuous information like physical conditions or satellite imagery, while vector data sets describe points, lines, or areas. In this study, raster data sets are used for oceanic conditions and bathymetry, while vector data sets describe regions of potential conflict and administrative boundaries. Current speed, dissolved oxygen, temperature, and salinity are used to determine the carrying capacity. Significant wave height and wave energy period are used to determine the wave power potential, which along with distance to port is used in the cost model. Bathymetry data, regions with other active industries, and restricted areas are used to constrain the feasible area. Together, these data sets are used to evaluate the location-dependent costs for each site and identify potential conflicts, as discussed in sections 5.2 and 5.3.

The data in this case study is sourced from several organizations that have publicly available GIS data including the Bureau of Ocean Energy Management (BOEM), the National Oceanic and Atmospheric Administration (NOAA), the National Renewable Energy Lab (NREL), the Northeast Ocean Data Portal (NODP), and the United States Census. Tables 1 and 2 contain an overview of the information used in the case study including the data type and file source. Section 4.1 explains the steps taken to standardize these different data sets which includes file conversion, interpolation, clipping, and re-projection. Preprocessed versions of each of these data sets are hosted on Zenodo at <https://zenodo.org/records/10140826>.

It is important to select data that is a good fit for the study, especially when multiple sources are available. With significant wave height and wave period, for example, an older raster data set of annual averages from NREL is chosen because it provides continuous information across the region and is available in a format that is readily compatible with GIS. NOAA's National Data Buoy Center, another possible option, could have provided the same information but would have limited the analysis to the few locations where buoys already exist and would have required more processing to integrate into the model. In other cases, available data sets may be limited by resolution or region. An older bathymetry data set, for example, is selected because it provides a high resolution across the entire study scope while more recent surveys are limited to a smaller region.

3.3. Software selection

Software is selected for this work with the intention of being accessible to a wide range of applications and users who might benefit from MSP. As a result, only open-source software is used in the final process. GIS software is used for basic processing and visualization of results including the layout of published maps. QGIS is used as the main GIS software because of its widespread availability and complete set of processing tools. QGIS unfortunately lacks the ability to process certain proprietary data types from ArcGIS, the current industry standard, but is otherwise a capable and free option. Python, along with the GeoPandas package, is used to handle more complex modeling such as the carrying capacity and cost functions which would be difficult in GIS software alone. For these cases, a Python package is created

Table 1: Raster data sets that are included in the study, including those relating to environmental conditions, wave energy potential, bathymetry, and distance to port. Source and approximate resolution are also noted.

Name	Unit	Notes	Source
Current speed	m/s	Finite volume community ocean model (FVCOM) annual climatology, 0.002° resolution downsampled to 0.004°	Northeast Ocean Data Portal and Shmookler (2016)
Dissolved oxygen	mg/L	Annual climatology, interpolated from vector data with 1° resolution to a raster with 0.015° resolution	National Centers for Environmental Information (2019)
Salinity	PSU	Annual climatology, interpolated from vector data with an irregular but roughly 0.1° resolution to a raster with 0.01° resolution	National Centers for Environmental Information (2019)
Temperature	°C	FVCOM annual climatology, 0.002° resolution	Northeast Ocean Data Portal and Shmookler (2016)
Wave height	m	51-month Wavewatch III hindcast, 0.067° resolution	National Renewable Energy Laboratory (2011)
Wave period	s	51-month Wavewatch III hindcast, 0.067° resolution	National Renewable Energy Laboratory (2011)
Bathymetry	m	0.0007° resolution, downsampled to 0.003°	National Geophysical Data Center (1990)
Distance to port	m	0.005° vector generated from vector of principal ports	Office for Coastal Management (2019)

Table 2: Vector data sets that are included in the study, including those relating to conflicting industries, restricted areas, and administrative boundaries.

Name	Notes	Source
Fishing traffic	Generated using raster from automatic identification system (AIS) transponders	Fontenault (2022)
Marine protected areas		National Marine Protected Areas Center (2020)
Military zones	Includes danger zones, restricted areas, submarine transit lanes, and testing areas	Northeast Ocean Data Portal et al. (2016); Office for Coastal Management (2022)
Offshore wind	Includes wind leases, planning areas, and existing farms	Northeast Ocean Data Portal (2015); Bureau of Ocean Energy Management (2023); Northeast Ocean Data Portal (2010)
Shipping lanes		Office of Coast Survey (2015)
State, federal waters		Office for Coastal Management (2018)
USA major cities		ESRI (2023)

to interface between the main model and the individual GIS data sets, as demonstrated in section 5.

4. QGIS processing and analysis

4.1. *Preprocessing data*

Several preprocessing steps are necessary to standardize downloaded GIS data files and prepare them for further mapping and analysis. These include occasional file conversion to a QGIS-compatible format, vector interpolation for environmental conditions, clipping data sets to the study scope, and reprojection to either WGS 84 or WGS 84 / UTM Zone 19. More thorough instructions to complete these steps in QGIS are provided in Appendix A.

4.2. *Raster analysis*

Although most analysis for this case study is done within the Python model shown in section 5, there are several helpful functions in QGIS that can aid in understanding and visualizing the data. For this study, two are used: generating contours to display the range of oceanic conditions, and highlighting regions that meet certain conditions or constraints with Raster Calculator. Figure 4 shows all raster data sets used in the case study, including environmental conditions used to identify favorable conditions for a certain species, average wave period and height to estimate WEC power output, and bathymetry and distance to port which further constrain feasible sites and affect the cost. The environmental conditions are also used to evaluate the carrying capacity of a location, which indicates how large a population can be sustained in a given environment. Generating contours and using the Raster Calculator in QGIS are both discussed in Appendix A.

4.3. *Vector analysis*

In this study vector data is used to represent conflicts, which QGIS can aid in identifying. It is often helpful to convert between raster and vector formats depending on the analysis needed. Areas with high fishing vessel traffic, for example, are excluded in this analysis and so a vector of regions that have high fishing traffic is first created using the raster input data. Vector data sets are the core of the conflict analysis used to identify overlapping industries, and each of the included data sets are pictured in figure 5.

Like raster files, vector data sets are later loaded into Python, but preliminary maps of conflicts can also be generated in QGIS to identify and highlight potential issues early on. Figure 6 demonstrates this technique using the data sets for wind lease areas and regions of high fishing traffic, and highlights the regions where these industries overlap and therefore could conflict. Note that although the regions highlighted in figure 6 include areas that had above-average fishing traffic in 2021, only areas with very high fishing traffic (over one standard deviation above the average) are considered infeasible farm locations in the Python model. This conclusion was determined after attending meetings hosted by the Bureau of Ocean Energy Management with stakeholders in the fishing and offshore wind industries. The fishing community is very protective of their fishing grounds and information about where they are is limited. Therefore, this assumption reflects a reasonable understanding of potential conflicts with fisheries and other industries.

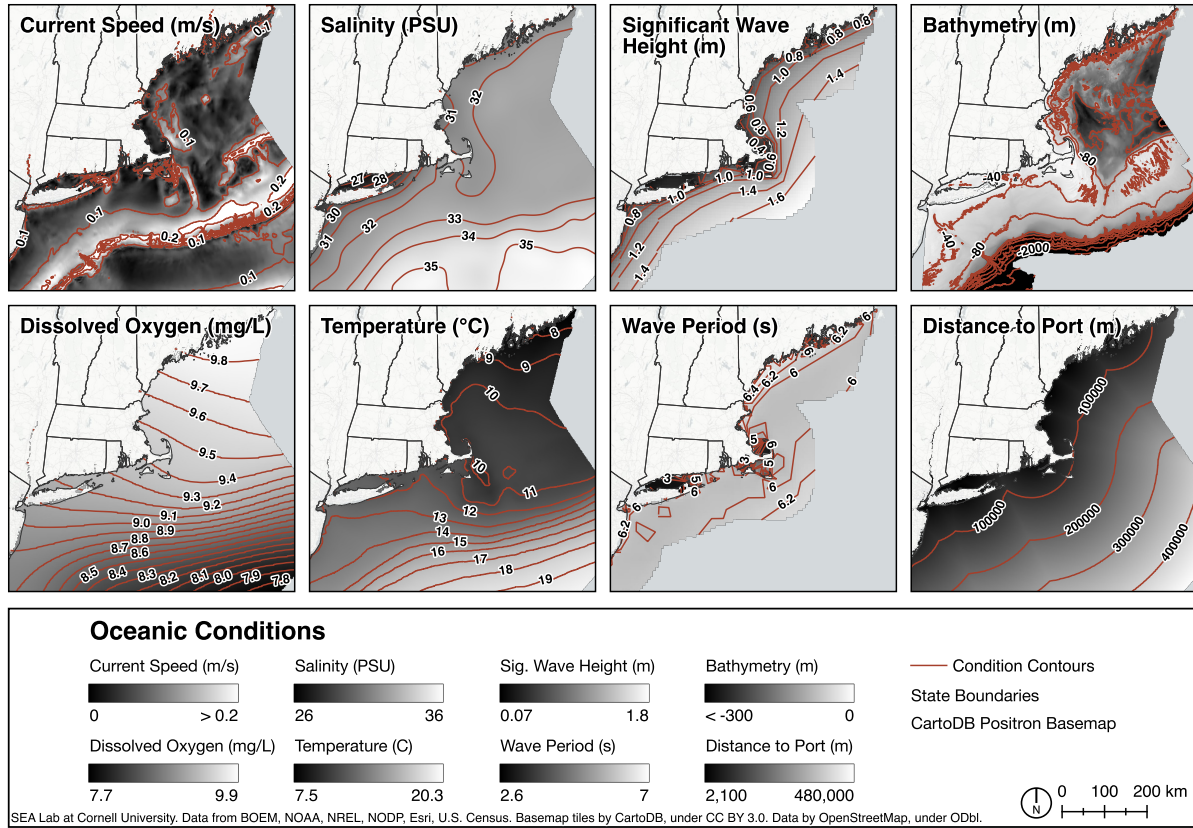


Figure 4: Raster data sets of conditions considered in the analysis with generated contours overlaid. Environmental conditions and bathymetry are used to identify feasible sites, while the wave climate and distance to port are used in the cost model.

5. Python integration and modeling

5.1. GIS-Python interface

Although QGIS is a powerful tool for the analysis and visualization of geospatial data, some functions like modeling and optimization are difficult in QGIS alone. For this reason, Python is used as an intermediary step for more complex analysis. Figure 7 shows the overall process for using both approaches where the Python optimization tool uses a “handler” object to query geospatial data processed in QGIS to evaluate the location-dependent costs of the farm. This handler and examples of its usage are available on the SEA Lab GitHub at <https://github.com/symbiotic-engineering/aquaculture>.

After completing the basic preprocessing described in 4.1, GeoPandas, Shapely, and Rasterio packages are used to process geospatial data in Python. First, a custom “handler” object is created in Python to handle the integration of the geospatial data sets with the Python model, which expects simple numerical values for conditions and flags for when there are potential conflicts. The handler first constructs a GeoPandas GeoDataFrame, which stores data and the results from the Python model in a format that can later be read again by QGIS. Conflict vectors are also loaded as separate GeoDataFrames, while condition rasters are loaded using Rasterio.

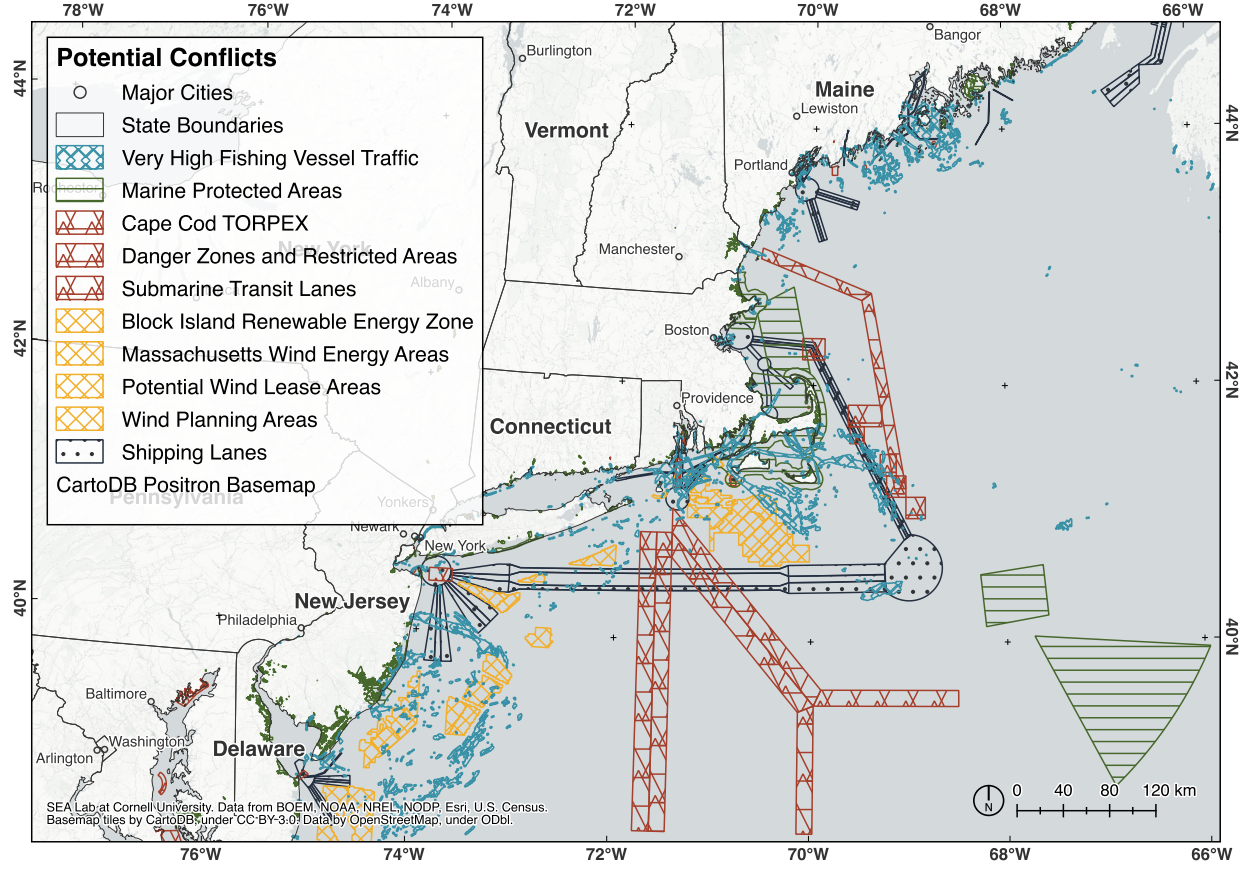


Figure 5: Data sets for all regions with conflicting industries or restricted areas that are excluded from the analysis, including shipping lanes, marine protected areas, and more.

The handler allows the model to query individual points by latitude and longitude and passes along the value at that point for each loaded condition raster. It then flags the point if overlaps with any of the vectors that have been loaded. One flag is used to identify conflicts, another is used to indicate whether the point queried is out of the study scope, and a third is used if all raster condition data sets exist at the given point. The handler then receives the result for a given point from the cost model and stores it in a GeoDataFrame. Although individual queries are helpful for an optimization approach, the handler can also query information for many points at once to fully populate a grid of potential sites. Finally, the GeoDataFrame with the model result is exported again as a GeoJSON file that can be loaded into QGIS to create final maps of the results.

5.2. Cost model

The cost model evaluates the costs associated with development of a WPAF at a given site, and is modeled entirely in Python. A brief explanation of the cost model as relevant to the WPAF case study is included here, but details about this function and the optimization process can be found in a previous paper by this author, Hasankhani et al. (2023b). In this study, the objective is to minimize the location-dependent cost of the WPAF, and the design variable is the WPAF deployment location which determines the environmental and

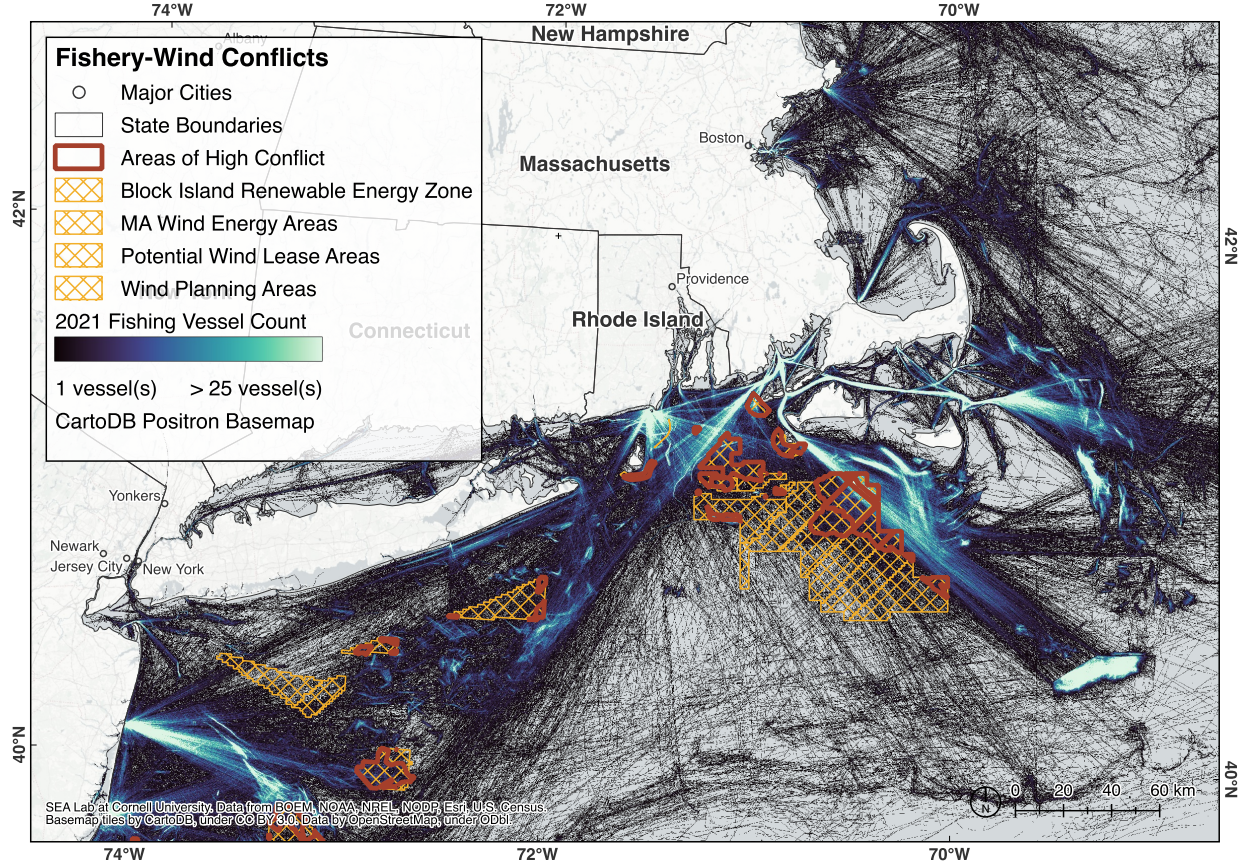


Figure 6: Fishing vessel traffic and offshore wind lease areas near Rhode Island with regions of overlap, and therefore a potential for conflict, highlighted.

geographic conditions used as inputs in the model.

The two WPAF cost terms that are the most dependent on the deployment location include the cost of the WECs and the cost of vessel travel associated with weekly trips to check the farm and restock the automatic feeders. The cost of WECs is determined by the availability of wave energy at a location and, from that, the number of RM3 WECs necessary to power a farm of a given size. The energy yield of the WEC is calculated considering the wave power density of the WPAF site and the capture width, which is the ratio of the power absorbed by the WEC to the wave power density of the site. This capture width is defined as the product of the physical dimension of the WEC and the hydrodynamic efficiency of the WEC, known as the capture width ratio. The capture width for an array of WECs is considered to be the sum of each individual WEC's capture width for this analysis. The wave power is found through the annual average of the significant wave height and wave period, as discussed in section 3.2. The model does not take into account the layout, direction, or near and far-field effects of the WECs and pens. Vessel travel cost to the WPAF is the second operating expense which increases for deployment locations further from the coast due to higher travel costs. This vessel travel cost is defined by the necessary travel time multiplied by the cost of labor and fuel. Though the total cost of the WPAF system depends on additional factors such as net pen design cost, feed barge cost, fish feed cost, and fingerling

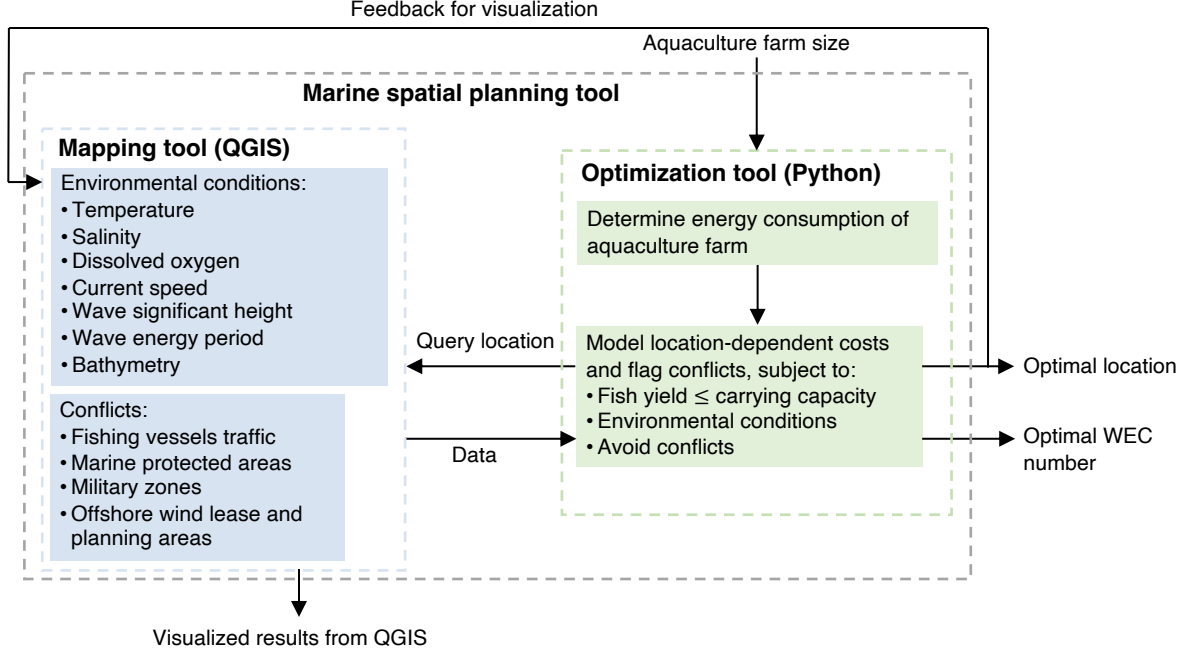


Figure 7: The analysis process between QGIS and Python for the marine spatial planning process.

cost, these remain constant for a designated size of aquaculture farm (e.g. five cylindrical net pens measuring 15 m in height and 30 m in diameter). These constant costs are therefore not modeled in this case study, but are the subject of future work. The location-dependent costs are modeled over the total lifetime of the project, including capital expenditures (CapEx) and operating expenses (OpEx). The objective function and total cost formulation is presented in equations 1 and 2 where $r = 0.07$ is the discount rate (FEMP, 2021) and t reaches the expected lifetime of 15 years.

$$\min_{\text{location}} \text{total cost}_{\text{WEC}} + \text{total cost}_{\text{vessel travel}} \quad (1)$$

$$\text{total cost} = \text{CapEx} + \sum_{t=1}^{15} \frac{\text{OpEx}}{(1+r)^t} \quad (2)$$

The CapEx and OpEx terms for WECs are defined by multiplying the number of WECs required to power the farm of a set size by the reference CapEx and OpEx of each RM3 WEC. These reference CapEx and OpEx for the RM3 are determined considering the economies of scale as detailed in (Neary et al., 2014). Values for costs that are not location-dependent are referenced in the results section in table 4. Constant capital expenditures include the net pen and feed barge, while constant operating expenses include fish feed and the fingerlings used to stock the farm at the beginning of each season. For this study, a harvest period of one year is considered, where the fingerlings are put in the net pens at a weight of 200g. Note that the cleaning costs of the net pens and feed barge are considered zero since they

are negligible compared to the capital cost (Innovasea, 2023).

A metric like levelized cost of energy is also used to calculate the cost per fish yield of a farm at a given site. This levelized cost of fish is calculated by dividing the total farm cost by the discounted fish yield over the lifetime of the farm, as shown in equation 3 where r and t are the same as in equation 2.

$$\text{levelized cost of fish} = \frac{\text{total cost}}{\sum_{t=1}^{15} \frac{\text{fish yield}}{(1+r)^t}} \quad (3)$$

It should also be mentioned that the cost analysis in this study is made per an assumption that the energy demand of the aquaculture farm is modeled as a constant annual value using a reference value for power per fish yield reported by Freeman et al. (2022). Hence, the energy demand is overestimated and considered constant per year, and hourly fluctuation of the power consumption of the aquaculture farm, such as an increase in energy demand while fish feeding, is not considered in this study. Furthermore, the uncertainty of the wave power, (i.e. the hourly data of wave significant height and wave energy period) is not considered in this study, and all the results are presented with the annual average wave data. Therefore, the cost of the WPAF, and specifically the cost of WEC, could change in future studies using high-resolution hourly data for aquaculture farm energy demand and wave power.

5.3. Constraints

The analysis assess for a variety of constraints to exclude sites that do not meet the feasibility requirements for WPAF development. These constraints include ensuring that a given site does not intersect with other offshore industries or restricted areas, that the necessary carrying capacity for Atlantic salmon is met, and that a suitable depth and environmental conditions within an acceptable range are present. These constraints are formulated in equations 4, 5, and 6 where CC_{O_2} refers to the carrying capacity considering oxygen availability.

$$\text{exclude conflicts with} \begin{bmatrix} \text{fishing vessels} \\ \text{shipping lanes} \\ \text{military zones} \\ \text{marine protected areas} \\ \text{offshore wind farms} \end{bmatrix} \quad (4)$$

$$\text{fish yield} \leq CC_{O_2} \quad (5)$$

$$\begin{bmatrix} \text{temperature}_{\min} \\ \text{salinity}_{\min} \\ \text{dissolved oxygen}_{\min} \\ \text{current speed}_{\min} \\ \text{depth}_{\min} \end{bmatrix} \leq \begin{bmatrix} \text{temperature} \\ \text{salinity} \\ \text{dissolved oxygen} \\ \text{current speed} \\ \text{depth} \end{bmatrix} \leq \begin{bmatrix} \text{temperature}_{\max} \\ \text{salinity}_{\max} \\ \text{dissolved oxygen}_{\max} \\ \text{current speed}_{\max} \\ \text{depth}_{\max} \end{bmatrix} \quad (6)$$

Intersection with existing industries and protected areas is evaluated directly by the GIS handler using the vector data sets of these regions. This information is then passed along with the environmental conditions from the raster GIS files at a selected site to the python model which evaluates the carrying capacity and environmental constraints alongside the objective function of location-dependent costs.

The carrying capacity is a measure of the amount of fish biomass that can be placed in the aquaculture farm while maintaining a healthy environment and is in this study determined using the current speed and dissolved oxygen (Stigebrandt et al., 2004). The carrying capacity of a row farm is formulated in equation 7 where O_{2in} is the average dissolved oxygen at the deployment site, O_{2min} is the minimum dissolved oxygen required for the fish, D_{pen} is the net pen diameter, H_{pen} shows the net pen height, U_{min} is the minimum current speed, Pe is the permeability of the farm, and DO_2 is the mean oxygen consumption rate per kilogram of fish production per day.

$$CC_{O_2} = \frac{86400(O_{2in} - O_{2min})n_{pens}D_{pen}H_{pen}U_{min}Pe}{DO_2} \quad (7)$$

Finally, the feasibility of the environmental conditions and bathymetry are evaluated for a given site. Table 3 lists the range of acceptable values for each of these constraints. The bathymetry constrain is set by the feasibility of mooring submersible net pens to the ocean floor, but the connections and power distribution between the WECs, net pens, and other equipment are not considered. The mooring requirements of the RM3 WEC of 40-100m (Neary et al., 2014) are considered but the requirements for submersible net pens of 40-75m are more limiting.

Table 3: Constraints for a sample offshore Atlantic salmon WPAF

Parameters	Description	Unit	Value	Source
T_{min}	Minimum temperature	°C	2	Pecherska (2019)
T_{max}	Maximum temperature	°C	20	Pecherska (2019)
sa_{min}	Minimum salinity	PSU	30	Pecherska (2019)
sa_{max}	Maximum salinity	PSU	35	Pecherska (2019)
O_{2min}	Minimum dissolved oxygen	mg/L	4.41	Pecherska (2019)
O_{2max}	Maximum dissolved oxygen	mg/L	-	
U_{min}	Minimum current speed	m/s	0.01	Pecherska (2019)
U_{max}	Maximum current speed	m/s	2	Pecherska (2019)
de_{min}	Minimum depth	m	40	Stakeholders
de_{max}	Maximum depth	m	75	Stakeholders

6. Results

In this section, the MSP results for a small WPAF with five net pens are presented. Although the conflict analysis significantly limits the number of feasible sites, a cost term is still initially calculated for each point in order to show overall trends, and the results are presented in figure 8. The results of the objective function calculating location-dependent costs across the region range from \$13.1M far from shore to \$4.0B in bays and sheltered areas near the coast where wave energy production is unrealistic.

Figure 9 shows the results of imposing different constraints on the WPAF model. Given the resolution of 0.1° latitude and longitude across this region, 7038 points are initially sampled, of which 3249 are offshore and only 1247 have data available for every condition in question. The number of feasible sites is further limited to 1182 feasible sites that meet acceptable environmental conditions, 529 sites with feasible bathymetry, 825 sites with no

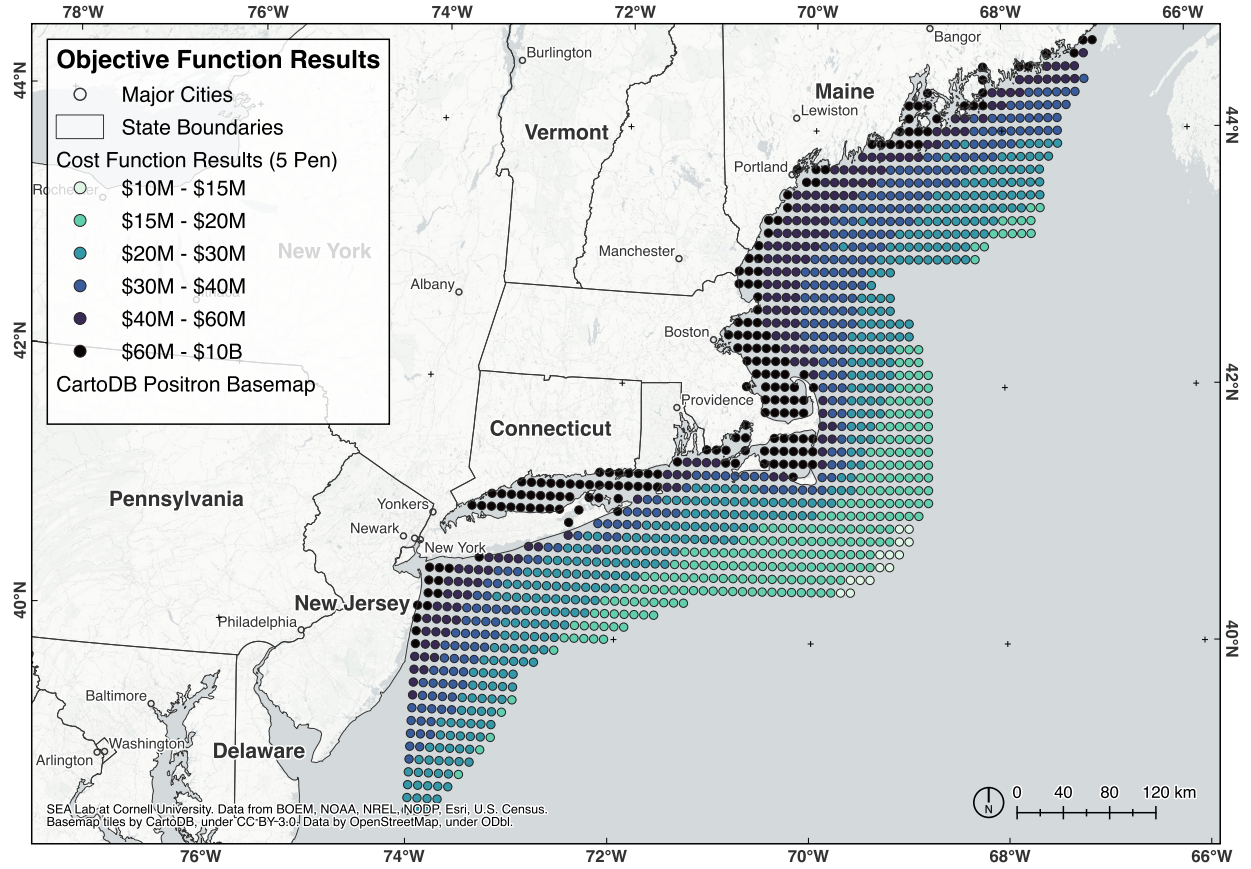


Figure 8: Results for the cost function (i.e. location-dependent costs over the lifetime of the farm) on all points with data available. Location-dependent cost is inversely correlated with distance from shore.

conflicts with industries or restricted areas, and 365 sites with sufficient carrying capacity. Together these constraints significantly narrow the feasible region and leave only 52 feasible sites ($\sim 4\%$) along the coast of Maine that meet all the requirements, as shown in figure 10.

Combining both the objective function and constraints yields several final sites that meet the stated requirements, and one optimal site with the lowest cost. For feasible sites, the objective function ranges from \$30.0M to \$3.0B and follows a similar trend as the overall results. Feasible sites are shown in figure 10, with figure 11 providing further detail near the optimal site. Both figures show sites color-coded by their value for levelized cost of fish. The small numbers next to each site on the figure denote the levelized cost of fish as a multiple of the cost of the optimal site.

The scatter plot, shown in figure 12, provides more detail on the results of the cost analysis and overall trends. The chart compares the effects of the two location-dependent cost terms in different subsets of the results. The diamond-shaped points show all non-dominated sites for the overall cost function without respect to constraints (figure 8) while the circular points show all sites that meet the constraints (figure 10). For each of these sets, a Pareto front and utopia point is shown, and the overall cost function is indicated by the color gradient. The utopia point refers the hypothetical ideal point that exists at the optimal values for each objective. The figure shows the dominance of WEC cost in the overall cost function as

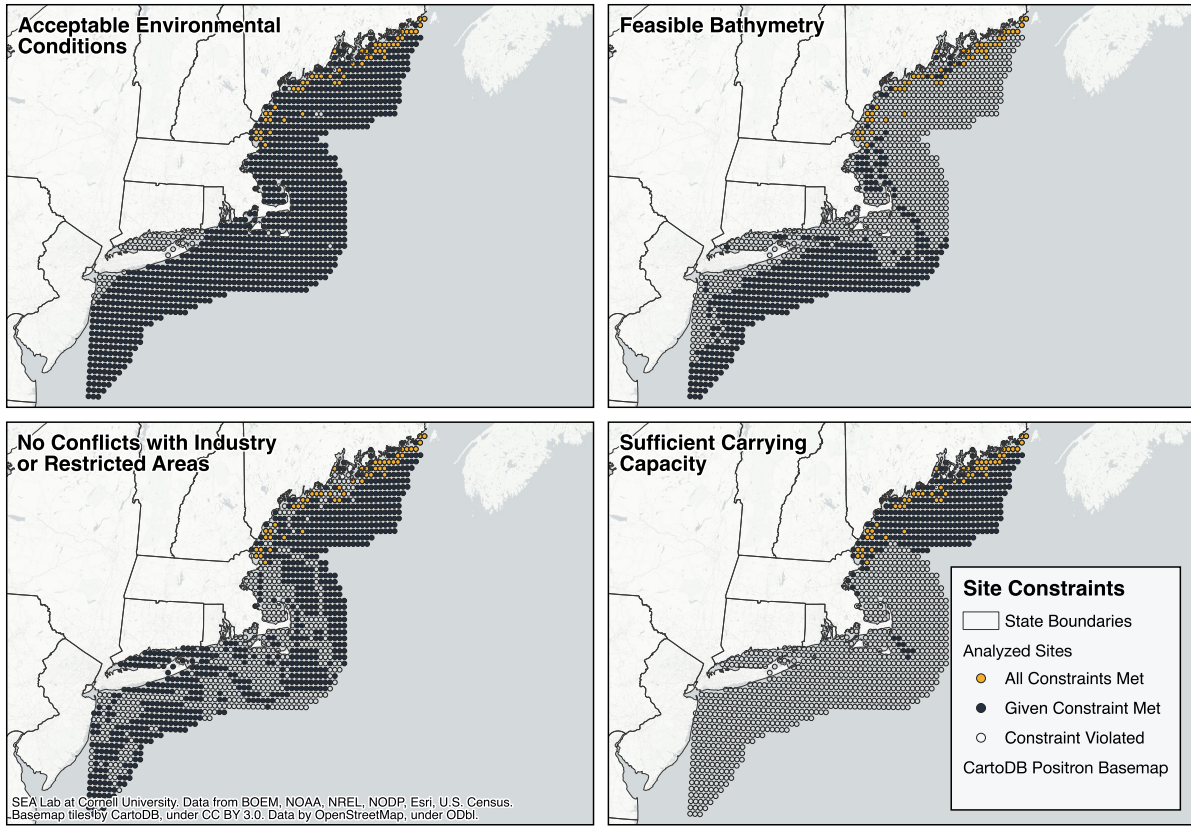


Figure 9: Potential sites with data available are evaluated for constraints including acceptable environmental conditions, feasible bathymetry, no conflicts, and sufficient carrying capacity.

the cheapest sites overall occur low on the WEC cost axis but vary only slightly with their position on the travel cost axis. The difference between feasible and overall non-dominated sites is also interesting. The cheapest feasible sites approach the overall Pareto front but fail to compete with the absolute cheapest sites because of the additional constraints.

An optimal site is identified southwest of Acadia National Park at 43.7°N 68.9°W. This site has location-dependent costs including WECs and vessel travel of \$30.0M and an overall cost of \$56.8M. A breakdown of all cost terms related to this site for a small WPAF with five cylindrical net pens is presented in table 4. Note that these costs are reported for the WPAF considering a lifetime of 15 years, and expected annual fish harvest from the farm.

It can be observed that WEC cost will account for more than half of the total cost of the WPAF, which highlights the importance of finding a location for this system with high wave power density and therefore a lower number of WECs. Using equation 3 and considering the total cost and an annual fish yield of 676 tonnes, the levelized cost of fish at the optimal site is estimated to be \$9.23 per kilogram. This unit price is marginally higher (~11%) than the current market rate which in 2023 placed salmon at \$8.28 per kilogram (Statista, 2024).

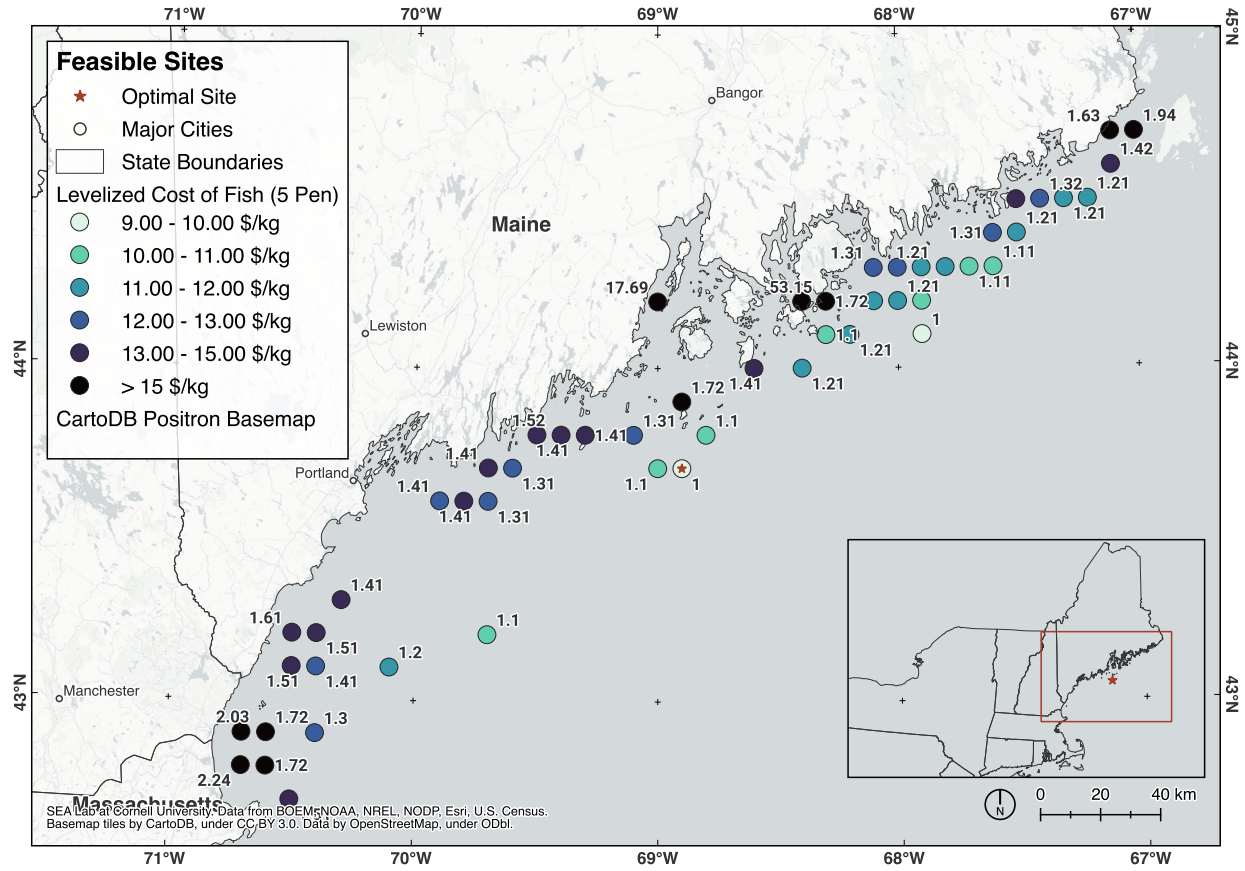


Figure 10: Sites that meet requirements of depth, carrying capacity, and lack of conflicts. Colors indicate the levelized cost of fish, and numbers indicate the cost multiplier relative to the optimal site.

Table 4: Overview of all cost terms for a sample small WPAF with five cylindrical net pens with a diameter of 30 m, height of 15 m, 15-year lifetime, and an annual fish yield of 676 tonnes at the optimal location of 43.7°N and 68.9°W (WEC cost accounts for CapEx and OpEx terms).

Cost term	Value [\$ millions]	Share [%]
WEC cost	29.45	51.8
Vessel travel cost	0.59	1.0
Net pen cost	5.30	9.3
Feed barge cost	3.73	6.6
Fish feed cost	12.8	22.5
Fingerling cost	4.94	8.7
Total cost	56.81	100

7. Discussion

Overall trends include a large amount of variation between the costs of each site despite relative proximity, driven in large part by access to wave resources. The decrease in cost further offshore demonstrates that location-dependent WPAF costs are dominated by the WEC cost, as opposed to the vessel travel cost which increases with distance from shore. The optimal site at 43.7°N 68.9°W, with location-dependent costs of \$30.0M is one of the

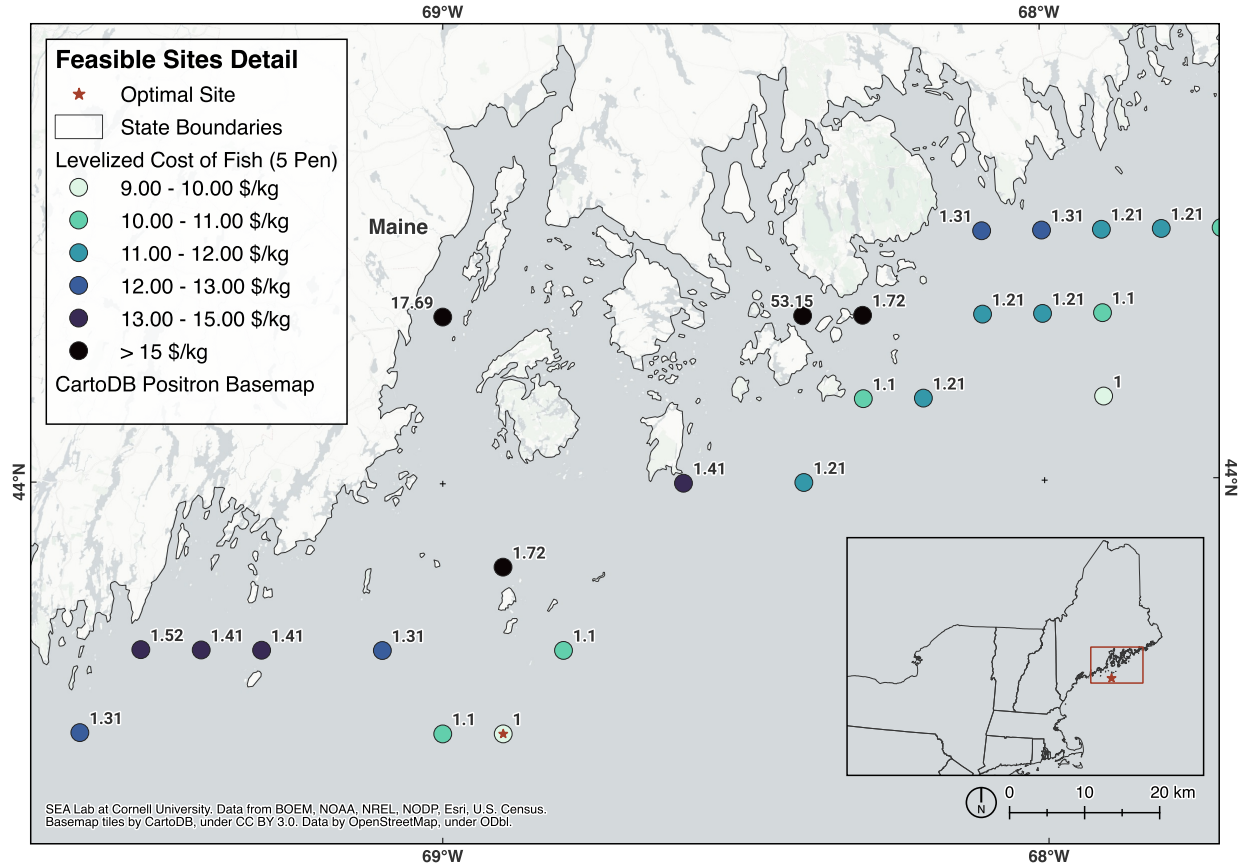


Figure 11: Detail of optimal sites and nearby feasible sites. Colors indicate the levelized cost of fish, and numbers indicate the cost multiplier relative to the optimal site.

furthest feasible sites from shore and has location-dependent costs several times cheaper than sites closer to land. Closer to shore, the cost increases significantly for sites in sheltered bays and other areas that would require many more WECs to power even a modest farm. This trend by far outweighs factors like the increased travel costs for deployment locations further from shore, although there are certain limits due to increasing depth and other constraints. The main takeaway from this cost analysis is that it is worthwhile to consider deployment locations farther offshore to decrease the WPAF cost by decreasing the number of required WECs. At these locations, the model estimates a levelized cost of fish near current market rates. Although this may indicate that the model is within the ballpark of actual costs, the cost model currently lacks enough detail to draw further conclusions or to make comparisons with market rates. The cost model used in this study does not include all cost components and instead focuses on those that change with location, such as distance to shore. The result is a relative, rather than absolute, metric intended to enable a comparison of different sites within the same study.

The conflict analysis also reveals the difficulty in finding a feasible site for a WPAF, especially given the number of other oceanic activities and the number of areas that do not meet the required bathymetry or carrying capacity. The final results end up being further north than perhaps expected, far away from many of the areas where current activities

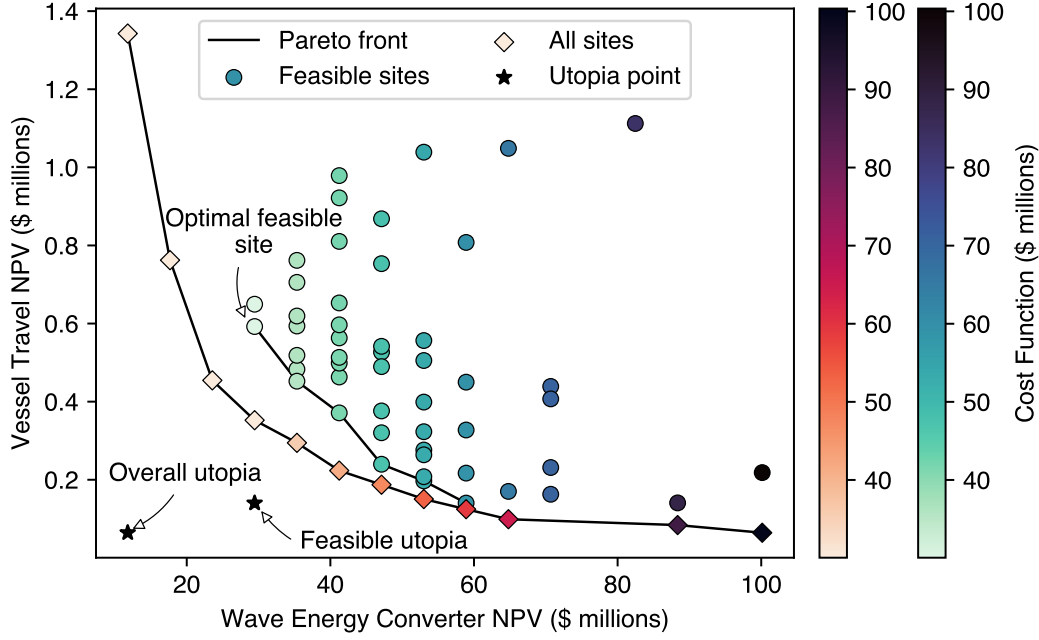


Figure 12: Results of the vessel travel and WEC cost function for feasible sites (circles), and overall results regardless of whether they meet the constraints (diamonds). Note that sites with excessive costs (\$600M and above) are not shown on plot.

like fishing and offshore wind development occur. In some cases, changes to the design or planning process may allow some of these constraints to be relaxed. Carrying capacity, for example, is the most limiting constraint in this case study and is strongly influenced by net pen size and fish stocking density. In this case study, these values are taken from current industrial net pen standards (Innovasea, 2023), but decreasing the size of the net pen or its stocking density would increase the number of feasible points, albeit at the cost of decreased yield. Conflicts with certain offshore areas, like military zones, may never be feasible while others, like wind farms, may allow for co-location in the future as potentially synergistic relationships are better understood. Future work investigating this synergy could increase the number of feasible points for the WPAF given the possibility of co-locating the wind farm and WPAF at the same site.

Existing WPAF studies demonstrate similar methodologies and trends, although it is difficult to compare results directly given that WPAFs remain a relatively new concept. A study by Clemente et al. (2023) investigates co-location potential at two sites along the Portuguese coastline using various farm designs. Although Clemente et al. (2023) do consider some similar factors including annual wave energy availability, a point absorber WEC as an energy source, and the feasibility of Atlantic salmon, their analysis is more focused on changing the design of the farm at a limited number of sites rather than analyzing many different sites with a single farm design. A study by Garavelli et al. (2022) is more similar to this study in that it focuses on siting and considers similar geographic factors including bathymetry, wave height, and marine protected areas. Their analysis yields similar results

to this study as they identify wave power density, bathymetry, and conflicts (in their case navigation routes and managed areas) to be key factors in determining favorable locations. However, they use a binary suitability score rather than a cost model making it difficult to directly compare the impact of these criteria on site selection.

8. Conclusion

Marine spatial planning is a topic of critical importance given the continued development of various offshore industries and our increasing reliance on aquatic resources for food and energy. Careful planning of these resources is necessary to ensure their sustainable use and avoid conflicts with other existing and future industries that operate along our coastlines. This paper provided an overview of several MSP techniques using open-source software including QGIS and Python, alongside the application of those techniques to a case study in siting a wave-powered aquaculture farm.

The MSP techniques discussed include the process of selecting a scope and preparing data, analysis options within QGIS of both vector and raster data sets as they relate to marine energy applications, and the potential to integrate with more complex Python models using GeoPandas, Rasterio, and a “handler” object made for the model used in the case study. Using information on the wave climate, biological conditions, and various conflicts, several feasible sites for a wave-powered aquaculture farm were identified along the coast of Maine. A cost model was then used to select one optimal location southwest of Acadia National Park with location-dependent costs of \$30.0M for a five-pen farm. The optimal site has a leveled cost of fish of \$9.23 per kilogram, which is on par with current market rates. The analysis revealed the importance of identifying conflicts in the siting process early on, and the significance of wave energy availability, and therefore distance to shore, to the cost of a project.

Future work on the case study of a wave-powered aquaculture farm includes more in-depth analysis given time series data of conditions and consideration of energy storage within the WPAF to ensure a reliable power supply. Different layouts, directions, near and far-field effects, and park effects could also be integrated to provide more detailed modeling of WEC performance. The cost model could also be improved by adding terms related to the energy transfer between the WEC and aquaculture farm. An integrated multi-trophic aquaculture setup will also be considered which allows other species such as kelp and mollusks to grow alongside fish with the goal of creating mutualistic relationships between the different species. This could be coupled with an expansion of the carrying capacity model to include aspects like nutrient use and production in addition to oxygen depletion. Additional environmental metrics would be useful to integrate as well, including constraints on benthic habitat and areas with endangered species, and emissions savings over a diesel-powered farm. The MSP techniques and generated map layers from this study will also be integrated into a more general web-based mapping tool to make the work more accessible to the many stakeholders who could benefit from this kind of analysis. Finally, more outreach with stakeholders will be conducted to receive feedback on the usefulness of the existing analysis and more information on the issues they face in practice.

Acknowledgments

This work was supported in part by Sea Grant Regional Research Project No. R/ATD-18-NESG and the Engineering Learning Initiatives program at Cornell University. We would also like to thank Rebecca McCabe and Matthew Haefner; members of the Symbiotic Engineering and Analysis (SEA) Lab; and our industry collaborators CalWave Power Technologies, Innovasea, and Manna Fish Farms, for providing feedback and support throughout this study.

Data Availability

Code required to reproduce the findings in this study is available in the SEA Lab GitHub at <https://github.com/symbiotic-engineering/aquaculture>, and the relevant pre-processed data files are hosted on Zenodo at <https://zenodo.org/records/10140826>. Raw data files are publicly available from the sources cited in tables 1 and 2.

Appendix A. QGIS Instructions

This appendix contains a brief overview of specific QGIS instructions for the steps outlined in this paper for those interested in following a similar procedure for MSP analysis. The QGIS Training Manual (https://docs.qgis.org/latest/en/docs/training_manual/index.html) and associated documentation are also helpful guides which provide more detail and further instructions. The processes below correspond to and are further explained in sections 4.1, 4.2, and 4.3.

Appendix A.1. File Conversion

Conversion from an ArcGIS format, is only necessary for certain raster files distributed in the proprietary GeoDatabase (.gdb) format. Although QGIS can currently access vector data in these files, rasters must be loaded into ArcGIS and exported as GeoTIFF (.tiff) files to be readable by QGIS and other applications. This process is straightforward but unfortunately requires users interested in using data from organizations that publish data in GeoDatabases to have access to ArcGIS.

Appendix A.2. Vector interpolation

Certain data sets for environmental conditions are distributed in a vector format with many points containing measurements instead of as a continuous raster. For many analyses, having a continuous raster of conditions is beneficial, and interpolation can be used to approximate this from discrete measurements. In this study, the data used for dissolved oxygen and salinity are distributed as vector files, but are converted to rasters. From the processing toolbox (**Processing > Toolbox**), the **TIN Interpolation** tool can be used to convert interpolate a vector data set of point measurements into a continuous raster data set. **TIN Interpolation** allows the user to select the desired layer, the attribute that contains the desired measurement, and a reasonable resolution (as discussed in section 3.1) for the given study. The resulting raster is limited to the area bounded by the original points, so **r.fill.stats** in the processing toolbox can be used to extend the range of the raster and

smooth the results of the interpolation. The parameters of this operation will vary by the study scope and individual data set. For this study, each raster is extended past the shoreline to ensure all coastal waters could be analyzed, then clipped back to include only the study scope.

Appendix A.3. Clipping

Data is clipped to only include the scope of designated state and federal waters. This relies on a vector layer describing the study scope which, in this study, is the file with state and federal waters from NOAA in table 2. To clip raster layers, click **Raster > Extraction > Clip Raster by Mask Layer...** and select the correct vector layer as a mask. For vector layers, click **Vector > Geoprocessing Tools > Clip...** and select the same mask as the overlay layer. Both operations will create a temporary scratch layer of the results, which can be exported to a permanent file.

Appendix A.4. Re-projection

GIS data and maps use different projections to translate the three-dimensional globe into a two-dimensional image. This study uses WGS 84 (EPSG:4326), a very common CRS, to standardize all downloaded data because of its simplicity, and so that each data set uses units of degrees in latitude and longitude. WGS 84 / UTM Zone 19 is used for final maps exported from QGIS, which is tailored for the specific region of the earth included in the scope and minimizes distortion in that area. Layers can be re-projected during the export process. Simply right-click and select **Export > Save Feature As...**, then select the desired projection (e.g. WGS 84) as the CRS. The CRS for final maps (e.g. WGS 84 / UTM Zone 19) is set later in the item properties of a map element in a layout, and does not need to match the CRS of individual layers.

Appendix A.5. Contour generation

Contours are generated via **Raster > Extraction > Contour....** An input layer can be selected alongside an interval size between each line, which should be picked based on the range of values in the particular data set. The attribute name, which defaults to **ELEV**, is the name of the field in the contour data set with measurement values. After generating contours, it can be helpful to style them or add labels in **Layer Styling > Labels** or in some cases filter out some the contours that are shown on the map. In the case of bathymetry, for example, the zero-value contour is filtered out along with many of the deeper regions where contours become more tightly spaced along the continental shelf.

Appendix A.6. Reclassification

The Raster Calculator (**Raster > Raster Calculator...**) is useful for a many operations including reclassification of raster data sets. To reclassify about the mean as in the case of fishing traffic, identify the mean and standard deviation in the layer properties dialog. The code below is an example used to reclassify fishing data given a mean of 4.6 vessels and standard deviation of 23.1.

```
("2021 All Vessel Activity@1" - 4.6) / 23.1
```

This generates a new output layer with fishing data centered around the mean which can be easily displayed or converted to a vector file as in the case of a conflicts analysis. Raster Calculator tends to output somewhat messy files, but these problems can be addressed with some additional clipping and layer styling.

Appendix A.7. Polygonalization

Raster > Conversion > Polygonize... can be run given the input raster and band (the component of a layer with a specific measurement) to convert the raster to vector areas. Depending on the input data file, the resulting vector will likely appear rough and may contain island-like areas that are too small to be relevant for analysis on a larger scale. There are several processing tools to improve the generated vector including **Delete holes**, which can fill in small areas; **Add geometry attributes**, which can calculate the area of each region thus allowing very small regions to be filtered or deleted; and **Buffer**, which can be used to expand or contract regions and create a smoother outer edge than what is generated from the original raster pixels.

Appendix A.8. Intersection identification

To find the intersection between two vector layers, use **Vector > GeoProcessing Tools > Intersection** and select the layers in question. This generates a new layer of the intersection which can be stylized to highlight conflicts or other areas of importance.

References

- Peter Arbo and Phạm Thị Thanh Thủy. Use conflicts in marine ecosystem-based management - The case of oil versus fisheries. *Ocean & Coastal Management*, 122:77–86, March 2016. doi: 10.1016/j.ocecoaman.2016.01.008. URL <https://www.sciencedirect.com/science/article/pii/S0964569116300084>.
- Nathan Andrews, Nathan J. Bennett, Philippe Le Billon, Stephanie J. Green, Andrés M. Cisneros-Montemayor, Sandra Amongin, Noella J. Gray, and U. Rashid Sumaila. Oil, fisheries and coastal communities: A review of impacts on the environment, livelihoods, space and governance. *Energy Research & Social Science*, 75:102009, May 2021. doi: 10.1016/j.erss.2021.102009. URL <https://www.sciencedirect.com/science/article/pii/S221462962100102X>.
- Randall Bess and Ramana Rallapudi. Spatial conflicts in New Zealand fisheries: The rights of fishers and protection of the marine environment. *Marine Policy*, 31(6):719–729, November 2007. doi: 10.1016/j.marpol.2006.12.009. URL <https://www.sciencedirect.com/science/article/pii/S0308597X07000152>.
- NOAA Fisheries. Offshore Aquaculture and the Future of Sustainable Seafood | NOAA Fisheries. NOAA, October 2023. URL <https://www.fisheries.noaa.gov/feature-story/offshore-aquaculture-and-future-sustainable-seafood>. Archive Location: Southeast.

- Rebecca R. Gentry, Halley E. Froehlich, Dietmar Grimm, Peter Kareiva, Michael Parke, Michael Rust, Steven D. Gaines, and Benjamin S. Halpern. Mapping the global potential for marine aquaculture. *Nature Ecology & Evolution*, 1(9):1317–1324, September 2017. doi: 10.1038/s41559-017-0257-9. URL <https://www.nature.com/articles/s41559-017-0257-9>.
- Carlos V. C. Weiss, Bárbara Ondiviela, Raúl Guanche, Omar F. Castellanos, and José A. Juanes. A global integrated analysis of open sea fish farming opportunities. *Aquaculture*, 497:234–245, December 2018. doi: 10.1016/j.aquaculture.2018.07.054. URL <https://www.sciencedirect.com/science/article/pii/S0044848618304605>.
- Cecile Brugere. Can integrated coastal management solve agriculture-fisheries-aquaculture conflicts at the land-water interface? a perspective from new institutional economics. *Environment and Livelihoods in Tropical Coastal Zones: Managing Agriculture-Fishery-Aquaculture Conflicts*, July 2006. doi: 10.1079/9781845931070.0258. URL <https://www.cabidigitallibrary.org/doi/10.1079/9781845931070.0258>.
- Ghose Bishwajit. Fisheries and Aquaculture in Bangladesh: Challenges and Opportunities. *Annals of Aquaculture and Research*, 1, July 2014. URL https://www.researchgate.net/publication/316585813_Fisheries_and_Aquaculture_in_Bangladesh_Challenges_and_Opportunities.
- Peter C. Longdill, Terry R. Healy, and Kerry P. Black. An integrated GIS approach for sustainable aquaculture management area site selection. *Ocean & Coastal Management*, 51(8):612–624, January 2008. doi: 10.1016/j.ocecoaman.2008.06.010. URL <https://www.sciencedirect.com/science/article/pii/S0964569108000604>.
- V. Stelzenmüller, J. Letschert, A. Gimpel, C. Kraan, W. N. Probst, S. Degraer, and R. Döring. From plate to plug: The impact of offshore renewables on European fisheries and the role of marine spatial planning. *Renewable and Sustainable Energy Reviews*, 158:112108, April 2022. doi: 10.1016/j.rser.2022.112108. URL <https://www.sciencedirect.com/science/article/pii/S1364032122000375>.
- Jeremy Firestone, Christine Hirt, David Bidwell, Meryl Gardner, and Joseph Dwyer. Faring well in offshore wind power siting? Trust, engagement and process fairness in the United States. *Energy Research & Social Science*, 62:101393, April 2020. doi: 10.1016/j.erss.2019.101393. URL <https://www.sciencedirect.com/science/article/pii/S2214629619306553>.
- Talya ten Brink and Tracey Dalton. Perceptions of Commercial and Recreational Fishers on the Potential Ecological Impacts of the Block Island Wind Farm (US). *Frontiers in Marine Science*, 5:439, November 2018. doi: 10.3389/fmars.2018.00439. URL <https://www.frontiersin.org/articles/10.3389/fmars.2018.00439/full>.
- Bela Hieronymus Buck, Gesche Krause, and Harald Rosenthal. Extensive open ocean aquaculture development within wind farms in Germany: the prospect of offshore co-management and legal constraints. *Ocean & Coastal Management*, 47(3):95–122, January 2004. doi: 10.1016/j.ocecoaman.2004.04.002. URL <https://www.sciencedirect.com/science/article/pii/S0964569104000262>.

- B. H. Buck, G. Krause, T. Michler-Cieluch, M. Brenner, C. M. Buchholz, J. A. Busch, R. Fisch, M. Geisen, and O. Zielinski. Meeting the quest for spatial efficiency: progress and prospects of extensive aquaculture within offshore wind farms. *Helgoland Marine Research*, 62(3):269–281, September 2008. doi: 10.1007/s10152-008-0115-x. URL <https://hmr.biomedcentral.com/articles/10.1007/s10152-008-0115-x>.
- Antje Gimpel, Vanessa Stelzenmüller, Britta Grote, Bela H. Buck, Jens Floeter, Ismael Núñez Riboni, Bernadette Pogoda, and Axel Temming. A GIS modelling framework to evaluate marine spatial planning scenarios: Co-location of offshore wind farms and aquaculture in the German EEZ. *Marine Policy*, 55:102–115, May 2015. doi: 10.1016/j.marpol.2015.01.012. URL <https://www.sciencedirect.com/science/article/pii/S0308597X15000238>.
- Lara Wever, Gesche Krause, and Bela H. Buck. Lessons from stakeholder dialogues on marine aquaculture in offshore wind farms: Perceived potentials, constraints and research gaps. *Marine Policy*, 51:251–259, January 2015. doi: 10.1016/j.marpol.2014.08.015. URL <https://www.sciencedirect.com/science/article/pii/S0308597X14002310>.
- Lysel Garavelli, Mikaela C. Freeman, Levy G. Tugade, David Greene, and Jim McNally. A feasibility assessment for co-locating and powering offshore aquaculture with wave energy in the United States. *Ocean & Coastal Management*, 225:106242, June 2022. doi: 10.1016/j.ocecoaman.2022.106242. URL <https://www.sciencedirect.com/science/article/pii/S0964569122002186>.
- D. Clemente, P. Rosa-Santos, T. Ferradosa, and F. Taveira-Pinto. Wave energy conversion energizing offshore aquaculture: Prospects along the Portuguese coastline. *Renewable Energy*, 204:347–358, March 2023. doi: 10.1016/j.renene.2023.01.009. URL <https://www.sciencedirect.com/science/article/pii/S0960148123000095>.
- Jonathan Whiting, Lysel Garavelli, Hayley Farr, and Andrea Copping. Effects of small marine energy deployments on oceanographic systems. *International Marine Energy Journal*, 6(2):45–54, December 2023. doi: 10.36688/imej.6.45-54. URL <https://marineenergyjournal.org/imej/article/view/100>.
- Dina Silva, Eugen Rusu, and C. Guedes Soares. The Effect of a Wave Energy Farm Protecting an Aquaculture Installation. *Energies*, 11(8):2109, August 2018. doi: 10.3390/en11082109. URL <https://www.mdpi.com/1996-1073/11/8/2109>.
- Arezoo Hasankhani, Rebecca McCabe, Gabriel Ewig, Eugene Thome Won, and Maha N Haji. Conceptual Design and Optimization of a Wave-Powered Offshore Aquaculture Farm. In *The 33rd International Ocean and Polar Engineering Conference*, Ottawa, Canada, June 2023a. URL <https://onepetro.org/ISOPEIOPEC/proceedings/ISOPE23/All-ISOPE23/ISOPE-I-23-112/524501>.
- Arezoo Hasankhani, Gabriel Ewig, Rebecca McCabe, Eugene Thome Won, and Maha N Haji. Marine Spatial Planning of a Wave-Powered Offshore Aquaculture Farm in the Northeast U.S. In *OCEANS 2023 - Limerick*, pages 1–10, Limerick, Ireland, June 2023b.

doi: 10.1109/OCEANSLimerick52467.2023.10244332. URL <https://ieeexplore.ieee.org/document/10244332>.

Vincent S Neary, Mirko Previsic, Richard A Jepsen, Michael J Lawson, Yi-Hsiang Yu, Andrea E Copping, Arnold A Fontaine, Kathleen C Hallett, and Dianne K Murray. Methodology for Design and Economic Analysis of Marine Energy Conversion (MEC) Technologies. *Sandia National Laboratories*, page 262, March 2014. URL <https://energy.sandia.gov/wp-content/gallery/uploads/SAND2014-9040-RMP-REPORT.pdf>.

Qian Zhong and Ronald W. Yeung. Wave-body interactions among energy absorbers in a wave farm. *Applied Energy*, 233-234:1051–1064, January 2019. doi: 10.1016/j.apenergy.2018.09.131. URL <https://www.sciencedirect.com/science/article/pii/S0306261918314442>.

Scale Aquaculture AS. SeaFarm Feeder Bow 200, 2019. URL <https://scaleaq.com/product/seafarm-feeder-bow-200/>.

Innovasea. Innovasea, 2023. URL <https://www.innovasea.com/open-ocean-aquaculture/>.

Patrick Whittle. Haul of Atlantic cod, once abundant, reaches new low. *WBUR*, March 2022. URL <https://www.wbur.org/news/2022/05/10/maine-massachusetts-cod-fishing-industry-record-low-catch>.

Northeast Sea Grant. Northeast Sea Grant Consortium, August 2022. URL <https://www.northeastseagrant.com>.

Northeast Ocean Data Portal and Rachel Shmookler. FVCOM Annual Climatology for Temperature, Stratification, and Currents, February 2016. URL <https://www.northeastoceandata.org/files/metadata/Themes/Habitat/FVCOMAnnualClimatology.pdf>.

National Centers for Environmental Information. World Ocean Atlas 2018 Data Access, July 2019. URL <https://www.ncei.noaa.gov/access/world-ocean-atlas-2018/>.

National Renewable Energy Laboratory. Marine and Hydrokinetic Resource Maps and Data, October 2011. URL <https://www.nrel.gov/gis/maps-marine.html>.

National Geophysical Data Center. Bathymetry, January 1990. URL <https://www.northeastoceandata.org/data-download/>.

Office for Coastal Management. Principal Ports, May 2019. URL <https://www.fisheries.noaa.gov/inport/item/56124>.

Jeremy Fontenault. Fishing Vessel Transit Counts from - 2021 AIS, May 2022. URL <https://www.northeastoceandata.org/files/metadata/Themes/AIS/FishingAISVesselTransitCounts2021.pdf>.

National Marine Protected Areas Center. The MPA Inventory, 2020. URL <https://marineprotectedareas.noaa.gov/dataanalysis/mpainventory/>.

- Northeast Ocean Data Portal, Naval Facilities Engineering Command (NAVFAC) Atlantic, and Ecology and Environment, Inc. National Security Layers, 2016. URL <https://www.northeastoceandata.org/data-download/>.
- Office for Coastal Management. Danger Zones and Restricted Areas, October 2022. URL <https://www.fisheries.noaa.gov/inport/item/48876>.
- Northeast Ocean Data Portal. Wind Energy Areas, 2015 Massachusetts Ocean Management Plan, January 2015. URL https://www.northeastoceandata.org/files/metadata/Themes/EnergyAndInfrastructure/moris_om_wind_energy_areas_poly.htm.
- Bureau of Ocean Energy Management. Renewable Energy Leases and Planning Areas, 2023. URL <https://www.boem.gov/renewable-energy/mapping-and-data/renewable-energy-gis-data>.
- Northeast Ocean Data Portal. Rhode Island Renewable Energy Zone, August 2010. URL <https://www.northeastoceandata.org/files/metadata/Themes/EnergyAndInfrastructure/RenewableEnergyZone.htm>.
- Office of Coast Survey. Shipping Fairways, Lanes, and Zones for US waters from 2010-06-15 to 2010-08-15, December 2015. URL <https://www.fisheries.noaa.gov/inport/item/39986>.
- Office for Coastal Management. Federal and State Waters from 2010-06-15 to 2010-08-15, April 2018. URL <https://www.fisheries.noaa.gov/inport/item/54383>.
- ESRI. USA Major Cities, 2023. URL <https://hub.arcgis.com/datasets/esri::usa-major-cities/explore>.
- FEMP. 2021 Discount Rates. Technical report, DOE, April 2021. URL <https://www.energy.gov/femp/articles/2021-discount-rates>.
- Mikaela C. Freeman, Lysel Garavelli, Eloise Wilson, Mark Hemer, Michael Lochinvar Sim Abundo, and Leonard Edward Travis. Offshore Aquaculture: A Market for Ocean Renewable Energy. Technical report, Implementing Agreement on Ocean Energy System, April 2022. URL <https://www.ocean-energy-systems.org/publications/oes-documents/market-policy-/document/offshore-aquaculture-a-market-for-ocean-renewable-energy/>.
- Anders Stigebrandt, Jan Aure, Arne Ervik, and Pia Kupka Hansen. Regulating the local environmental impact of intensive marine fish farming: III. A model for estimation of the holding capacity in the Modelling-Ongrowing fish farm-Monitoring system. *Aquaculture*, 234:239–261, May 2004. doi: 10.1016/j.aquaculture.2003.11.029. URL <https://www.sciencedirect.com/science/article/pii/S0044848603008007>.
- Tetyana Pecherska. U.S. Offshore Aquaculture Potential in the Atlantic Ocean and Gulf of Mexico. In *AAG Annual Meeting 2019*, April 2019. URL <https://aag.secure-abstracts.com/AAG%20Annual%20Meeting%202019/abstracts-gallery/22695>.
- Statista. Salmon price index worldwide 2023, March 2024. URL <https://www.statista.com/statistics/1195271/price-salmon-price-index/>.